University of Venda

Aerial Radiometric Measurements at an old disused Phosphate Mine in the West Coast Fossil Park, South Africa

MASEGO MOTHAPO

PRESENTATION OUTLINE

- Introduction
- Background
- Aim
- Objectives
- Methods & Materials
- Results & Discussion
- Conclusion
- Acknowledgements

INTRODUCTION

- Phosphate mining: extraction and processing of phosphate rocks for agricultural and industrial use.
- Essential for fertilizer production, but associated with environmental and radiological impacts.
- Mining and processing can enhance NORM.
- The primary radionuclides of concern include U-238, Th-232, K-40 and their decay products (Ra-226, Pb-210, Po-210).
- The **distribution and concentration** of these radionuclides is influenced by geological and morphological characteristics of the study area.

BACKGROUND

History of the West Coast Fossil Park:

- •Site: Old phosphate mine at Langebaan (West Coast, South Africa).
- •Geology: Marine sands → rich fossil deposits → now a Fossil Park.

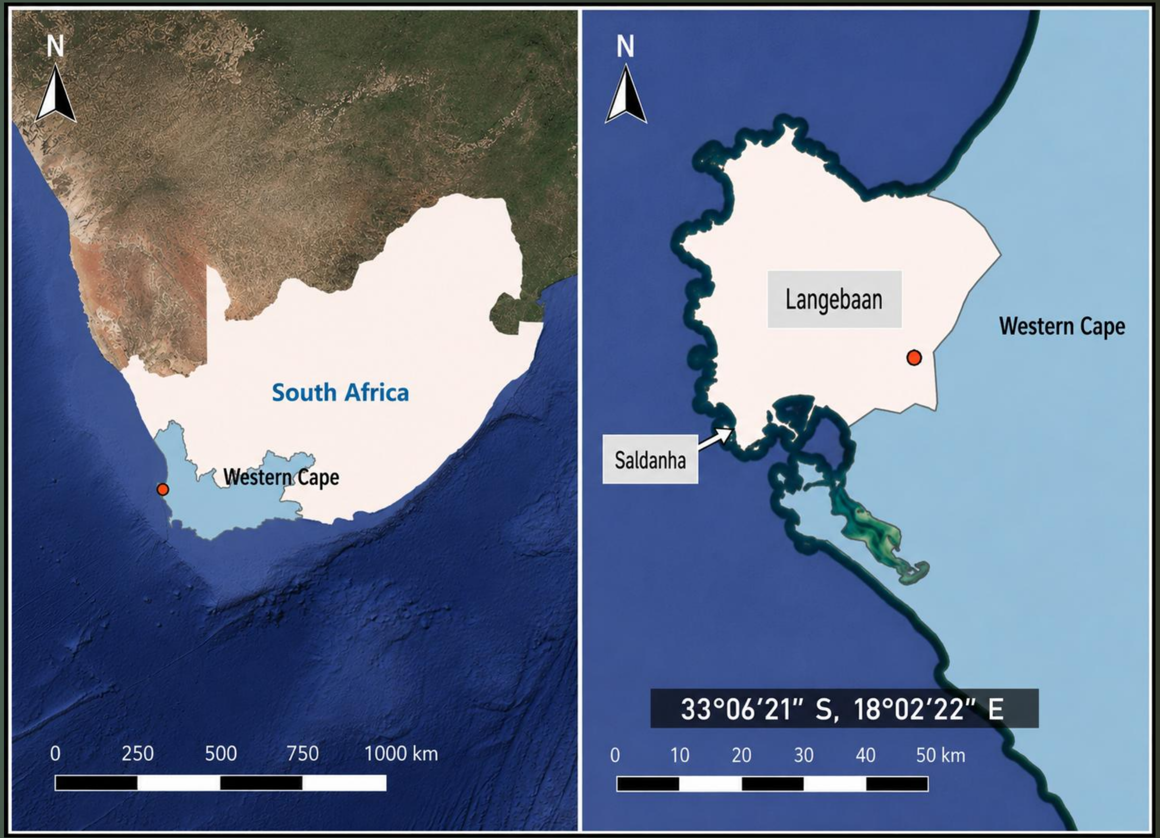

Figure 1: Location of the West Coast Fossil Park, Langebaan in the Western Cape, South Africa (adapted from Google Earth Pro, 2026).

AIM

To measure and map natural radioactivity in the soils of the West Coast Fossil Park, using a UAV.

OBJECTIVES

- To use a UAV to measure natural radionuclides (^{238}U, ^{232}Th, ^{40}K) in the soil.
- To map where these radionuclides are found and how their activity concentrations change across the site.
- To analyse radionuclide relationships using ternary diagrams and scatter plots.

METHODS & MATERIALS

- Area of Study:

The West Coast Fossil Park is at an old disused phosphate mine.

- System used for Measurements:

A DJI Matrice M300 RTK with 2x TB65 Li-ion batteries attached to a 3x3 enclosed NaI(Tl) scintillation detector with a photomultiplier tube (PMT), linked to an AMPTEK TB-5 Digital Tube Base, was used for radiometric survey at the West Coast Fossil Park

Figure 2: GRASS UAV System used for the radiometric measurements.

PREPARATIONS & CALIBRATION OF THE SYSTEM BEFORE LAUNCH

- Detector Calibration: Radium source, left 5 minutes for stabilization.
- Energy Peaks: Several channels aligned to specific energies of the decay daughters, 295 and 352 keV for ^{214}Pb, 609 and 1765 keV for ^{214}Bi.
- Fit: Quadratic fit to give an equation to change the channels to energy.
- Deviation values were less than 1, showing good calibration.
- Flight Plan: A pre-planning plot of the area was set in DJI Pilot 2 software, with a height of 5m, speed of 1m/s, and a sampling time of 5s.
- Launch: The drone was then launched with the set height, speed, and sampling time.

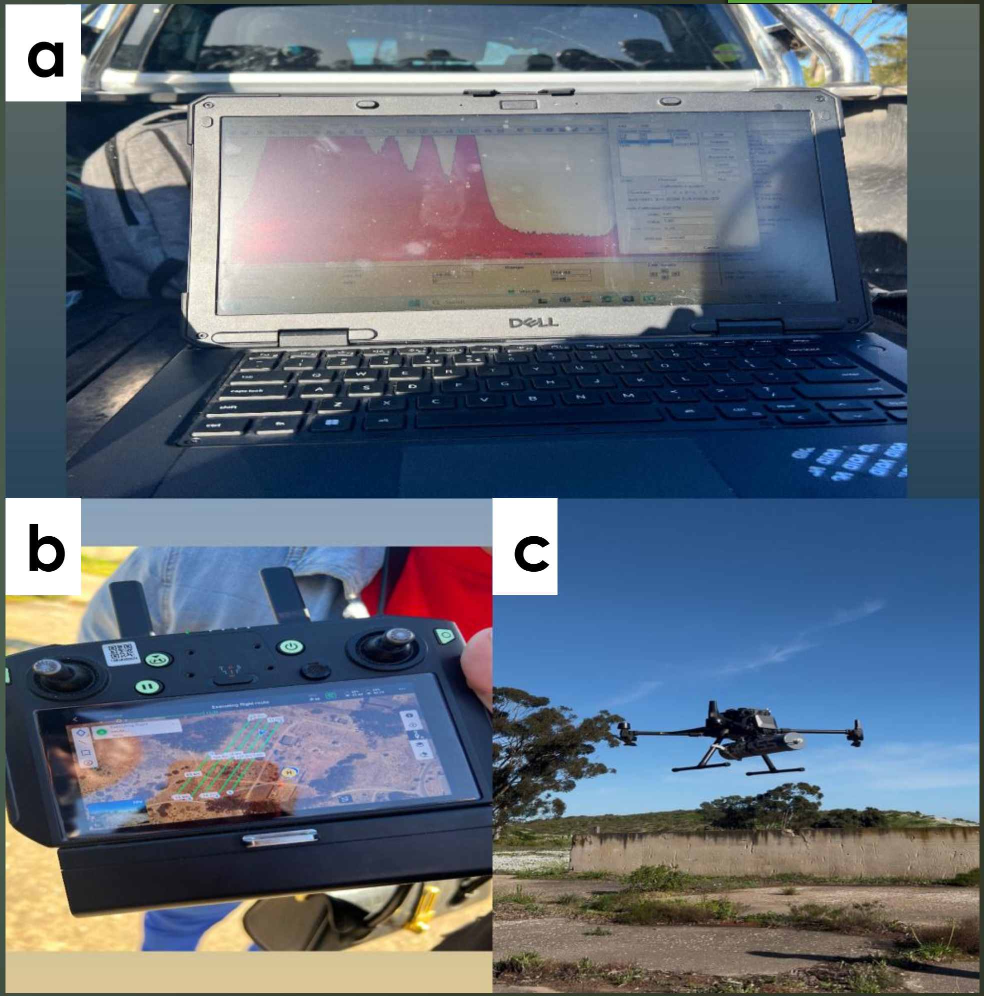

Figure 3: (a) Calibration spectrum showing channels and energies of different peaks and deviation values after a Quadratic fit.
(b) A pre-planning plot of the area using DJI Pilot 2 on the remote controller.
(c) UAV launching after calibration and pre-planning plot.

RESULTS & DISCUSSION

Spectrum Analysis:

- A Full-spectrum analysis was performed to examine the output of the radiation detector
- Main Energy Peaks (keV)

    U-238: 186, 295, 352, 609, 1765

    Th-232: 238, 338, 583, 911

    K-40: 1460

- Checked for drift and none was found.

Data Analysis:

- QGIS software and Excel Ternary plot were used for data analysis, plotting the maps, drawing scattered plots, and creating the ternary diagram

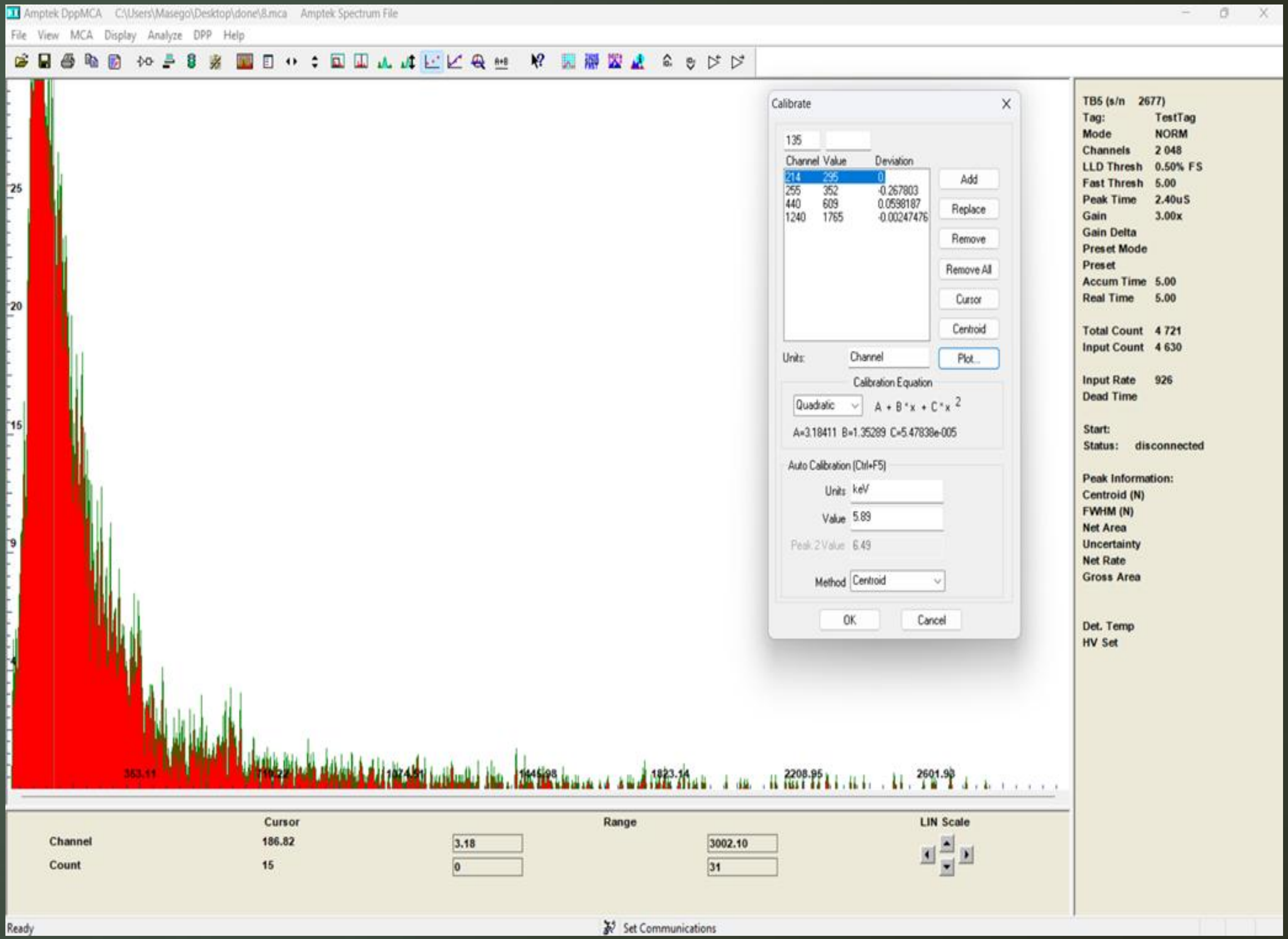

Figure 4: Spectrum showing the output of the radiation detector.

CONTINUATION OF RESULTS AND DISCUSSION

The colours represent different **Potassium Activity (Bq/kg)** concentration ranges:

- Dark Red = High Potassium Concentrations
- Light Red = Medium Potassium Concentrations
- White = Low Potassium Concentrations

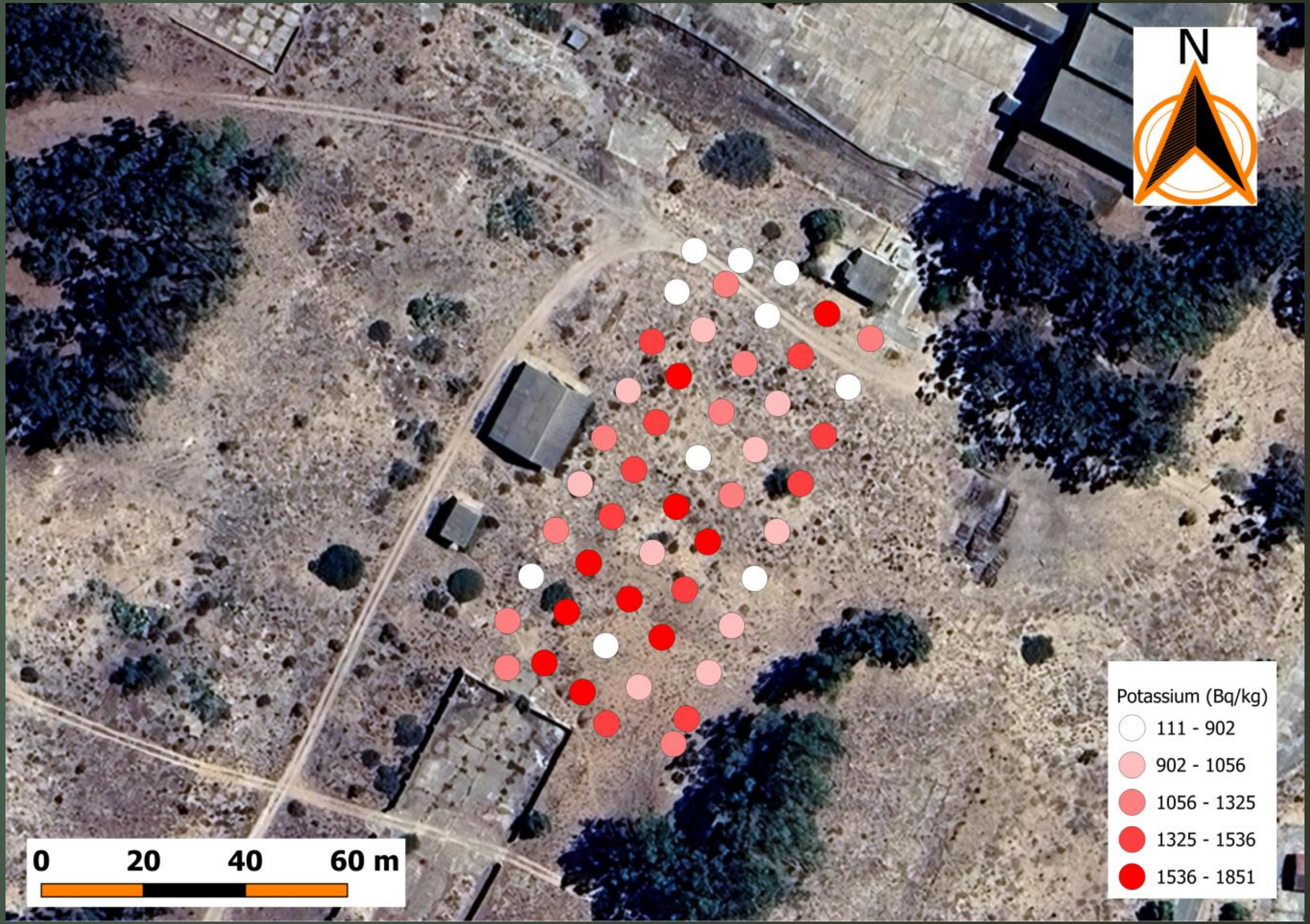

Figure 4: Distribution of potassium concentrations (Bq/kg) measured at discrete sampling points across the site. Each circle represents a sampling location, with colors corresponding to potassium activity levels ranging from 111 to 1851 Bq/kg.

RESULTS CON.

The colours represent different **Uranium Activity (Bq/kg)** concentration ranges:

- Dark Blue = High Uranium Concentrations
- Light Blue = Medium Uranium Concentrations
- White = Low Uranium Concentrations

Figure 5: Distribution of uranium concentrations (Bq/kg) measured at discrete sampling points across the site. Each circle represents a sampling location, with colors corresponding to uranium activity levels ranging from 93 to 318 Bq/kg.

RESULTS CON.

The colours represent different **Thorium Activity (Bq/kg)** concentration ranges:

- Dark Green = High Thorium Concentrations
- Light Green = Medium Thorium Concentrations
- White = Low Thorium Concentrations

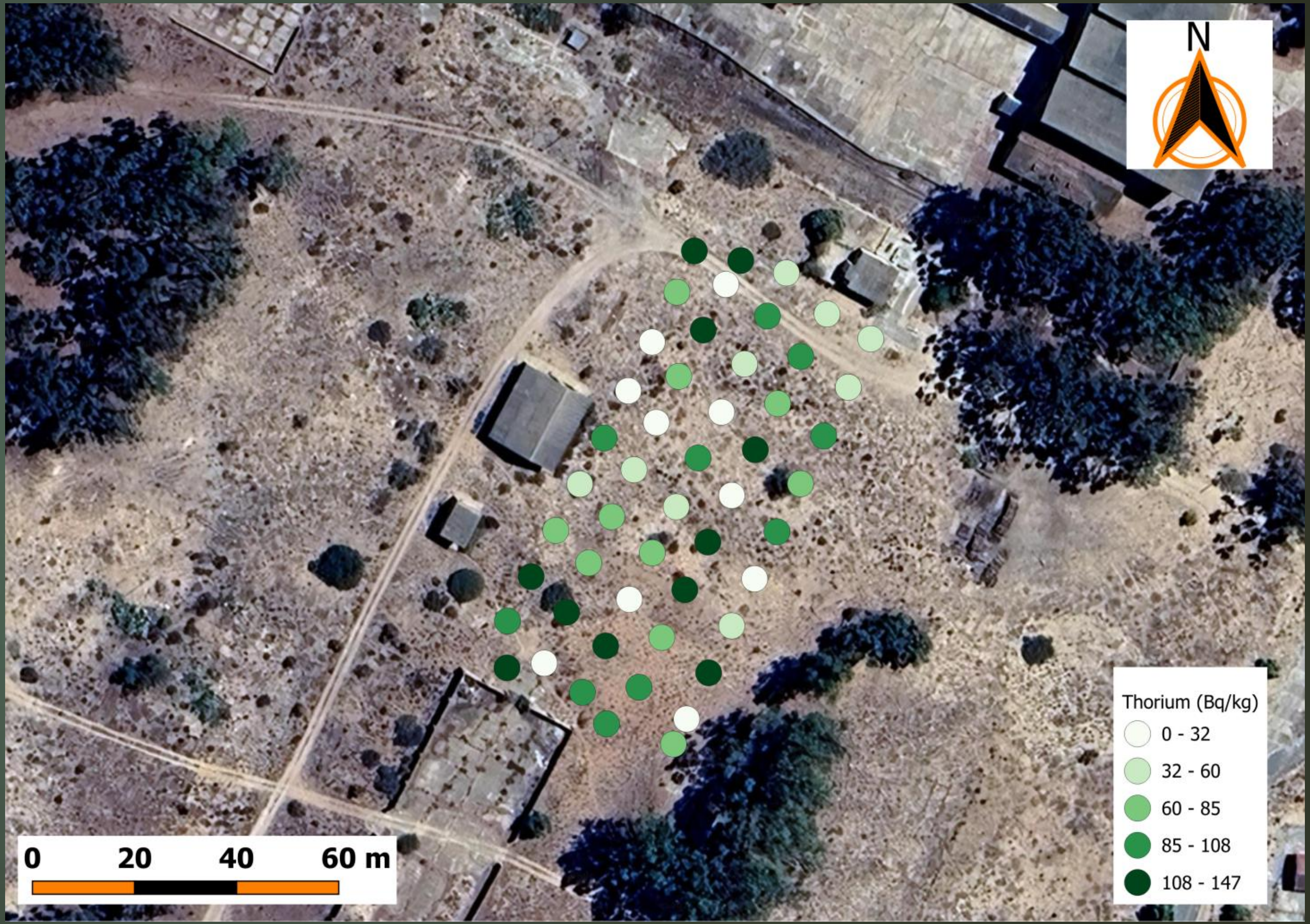

Figure 6: Distribution of thorium concentrations (Bq/kg) measured at discrete sampling points across the site. Each circle represents a sampling location, with colors corresponding to thorium activity levels ranging from 0 to 147 Bq/kg.

RESULTS CON.

The IDW (Inverse Distance Weighting) interpolation presents the potassium distribution, showing hotspots of higher activity.

Potassium (IDW Map)

- Dark Red = High Potassium Activity
- Light Red = Medium Potassium Activity
- White = Low Potassium Activity

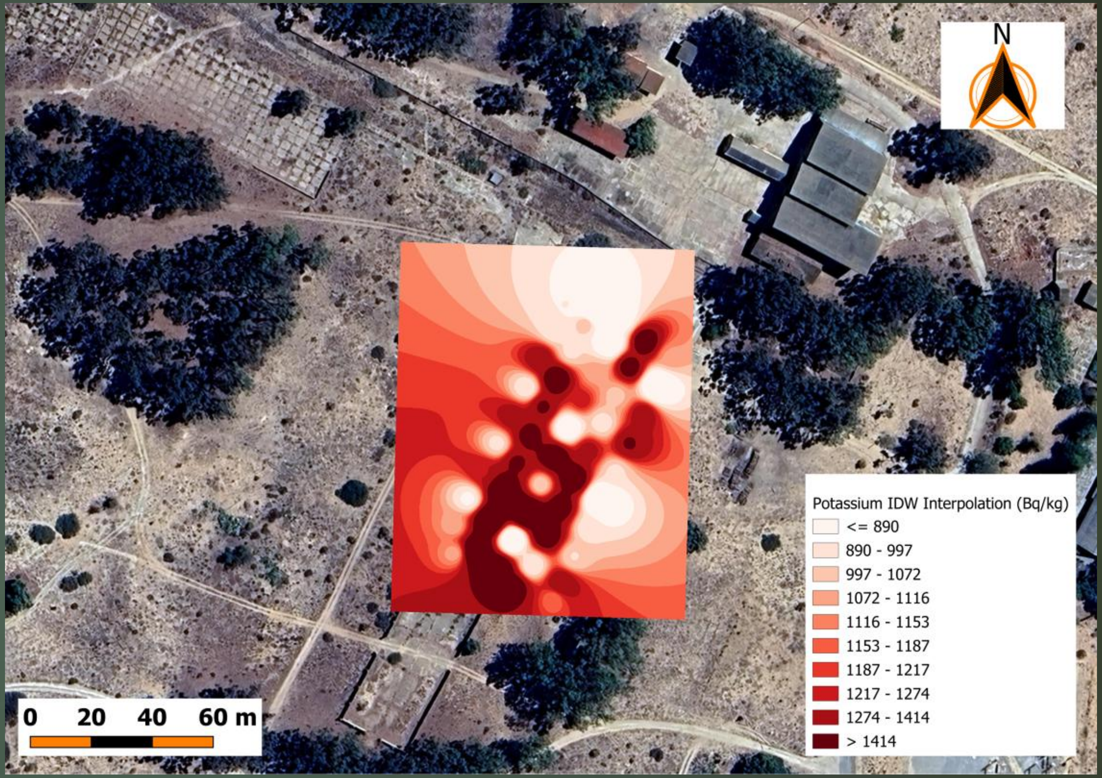

Figure 7: Potassium concentrations in (Bq/kg) across the study site interpolated using the Inverse Distance Weighting (IDW) method. Darker red shades represent areas with higher potassium activity (>1414 Bq/kg), while lighter shades represent lower activity (<=890 Bq/kg).

RESULTS CON.

The IDW (Inverse Distance Weighting) interpolation shows how uranium is spread around the area, showing hotspots of higher activity.

Uranium (IDW Map)

- Dark Blue = High Uranium Activity
- Light Blue = Medium Uranium Activity
- White = Low Uranium Activity

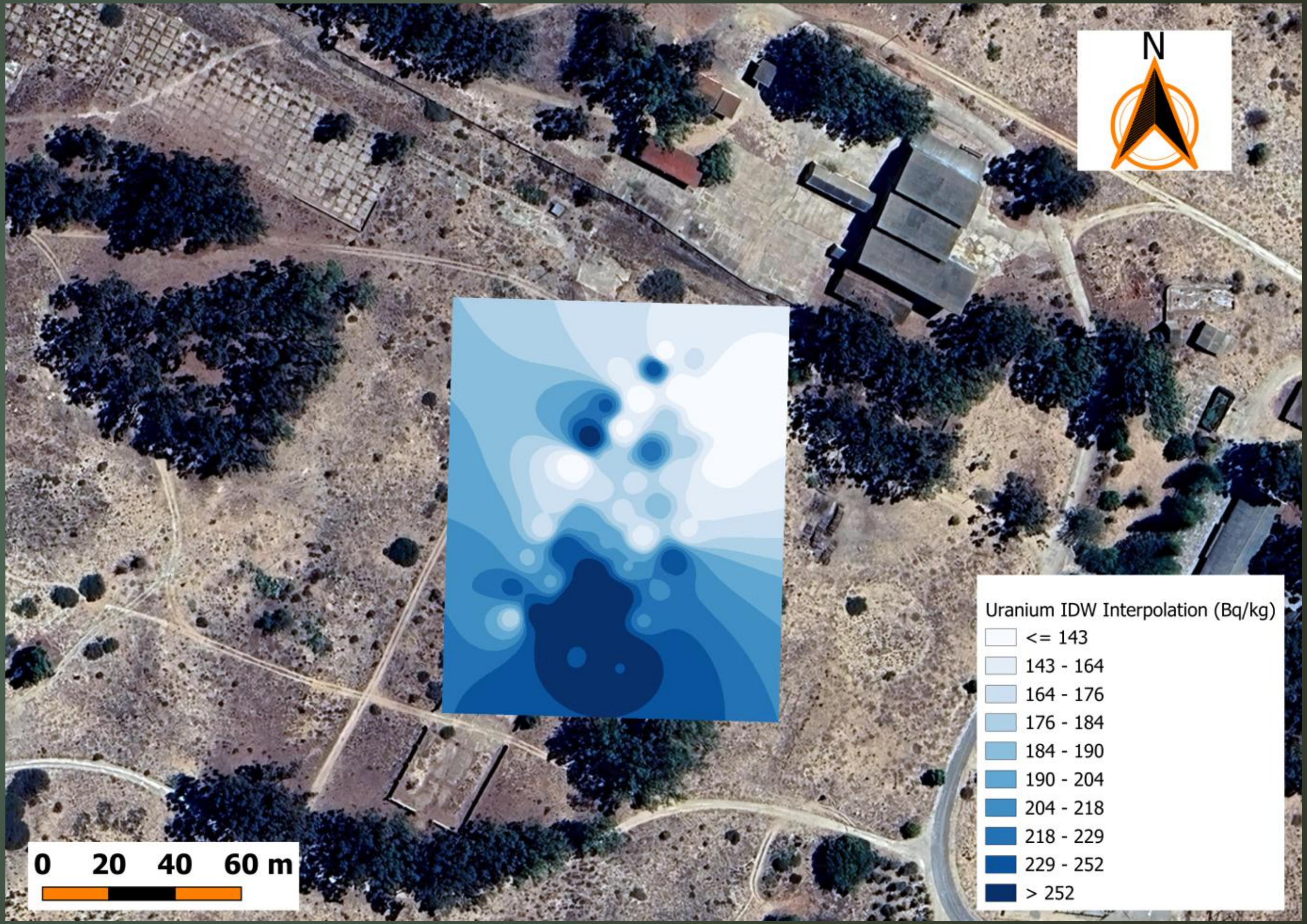

Figure 8: Uranium concentrations (Bq/kg) across the study site interpolated using the Inverse Distance Weighting (IDW) method. Darker blue shades represent areas with higher uranium activity (>252 Bq/kg), while lighter shades represent lower activity (<=143 Bq/kg).

RESULTS CON.

The IDW (Inverse Distance Weighting) interpolation shows how thorium spreads around the area, showing hotspots of higher activity.

Thorium (IDW Map)

- Dark Green = High Thorium Activity
- Light Green = Medium Thorium Activity
- White = Low Thorium Activity

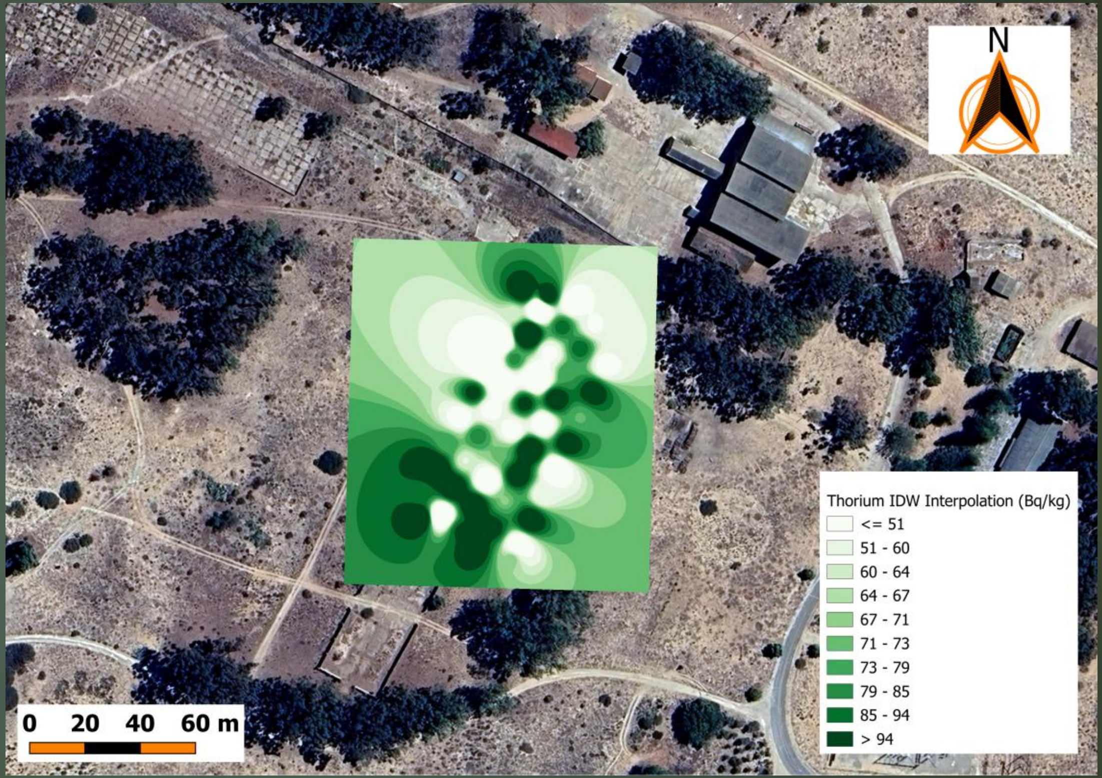

Figure 9: Thorium concentrations (Bq/kg) across the study site interpolated using the Inverse Distance Weighting (IDW) method. Darker green shades represent areas with higher thorium activity (>94 Bq/kg), while lighter shades represent lower activity (<=51 Bq/kg).

SCATTER PLOTS SHOWING THE RELATIONSHIPS BETWEEN URANIUM (U), THORIUM (TH), AND POTASSIUM (K) ACTIVITIES IN THE STUDY AREA

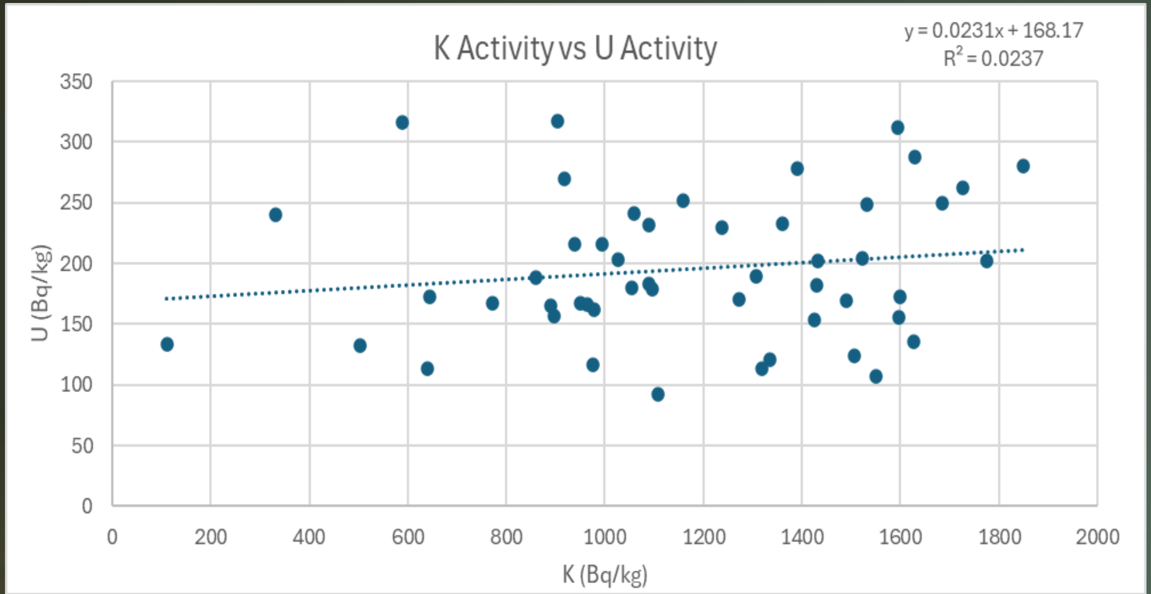

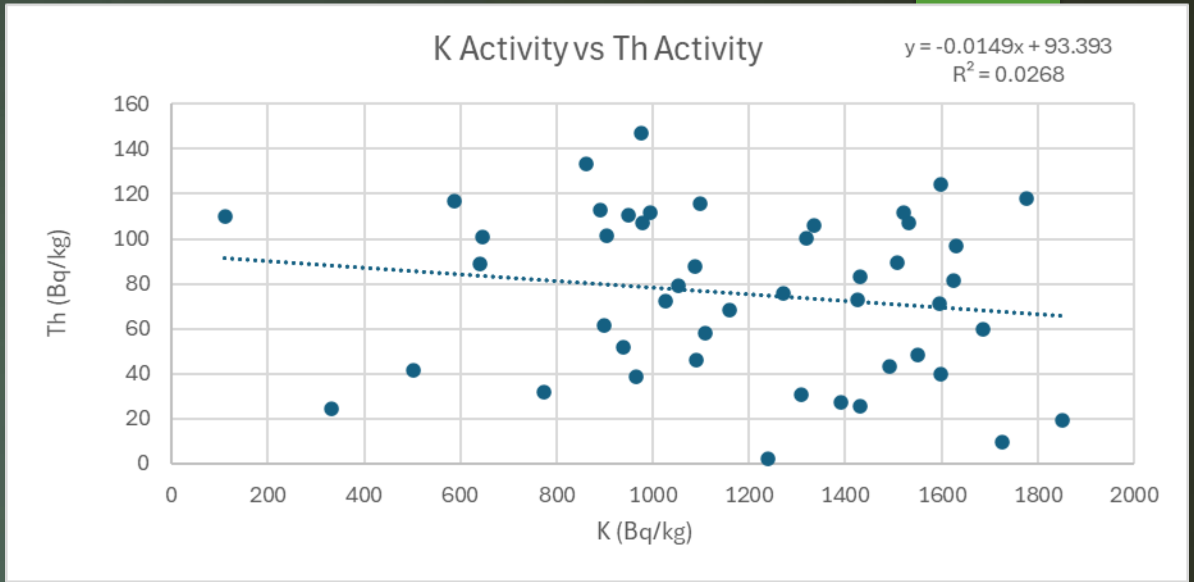

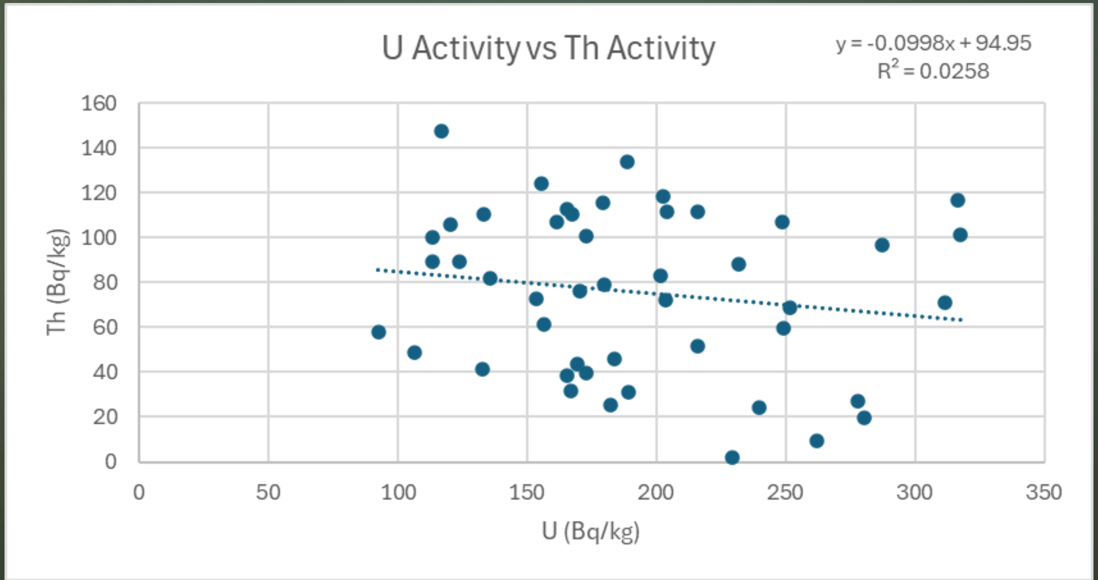

Figure 10: Scatter plots of radionuclide activities

RESULTS CON.

Ternary Diagram (K–U–Th)

- Shows the contribution of each radionuclide (K, U, Th) in the area.
- Points cluster near the center.
- Slight shift towards **U** → showing high contribution of uranium in the sample.

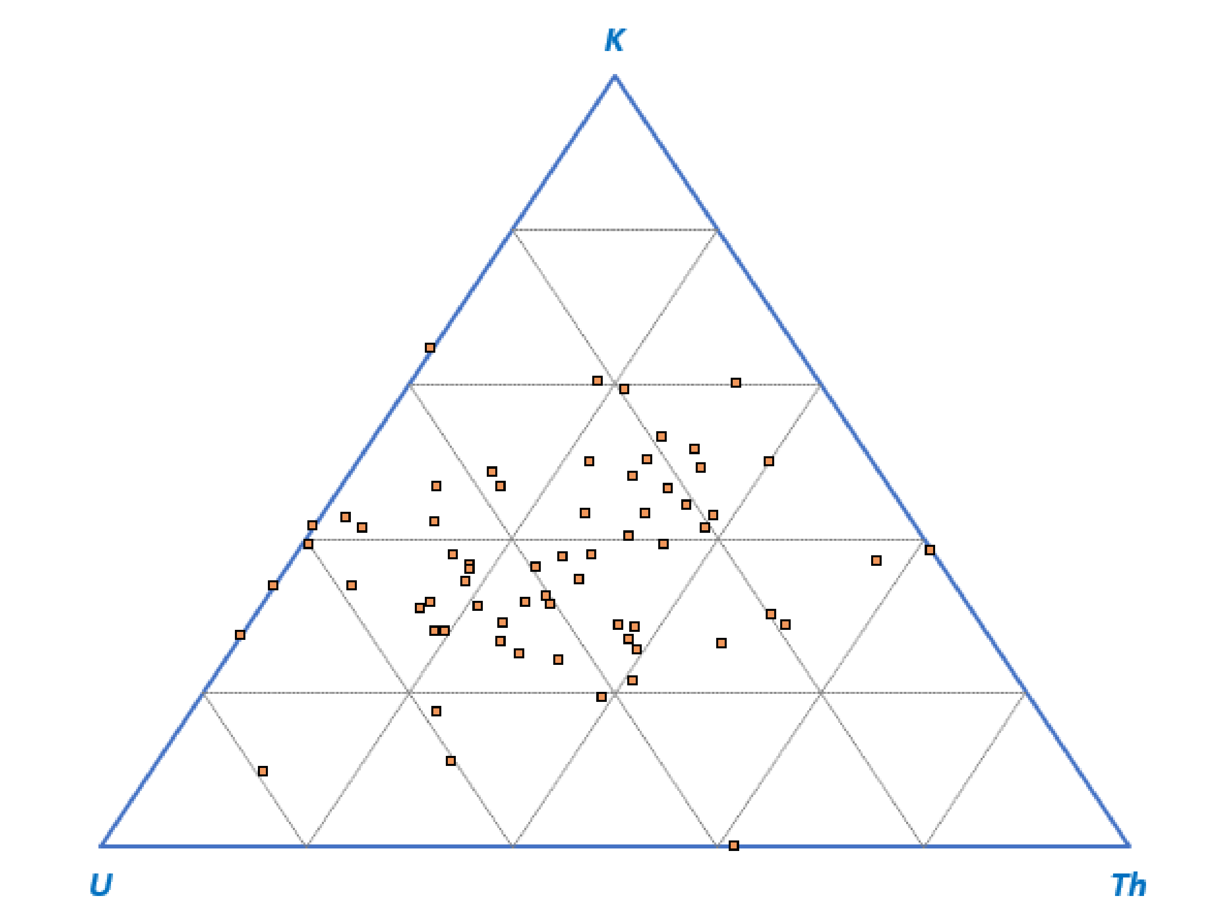

Figure 11:Ternary diagram showing the relative proportions of potassium (K), uranium (U), and thorium (Th) at sampling sites. Each point represents a sample, plotted according to the normalized contributions of the three radionuclides.

CONCLUSION

- UAV mapping and measurements of ^{238}U, ^{232}Th, ^{40}K in the soil was successful.
- Uranium (^{238}U) was identified as the radionuclide most strongly associated with the former phosphate mining activities, while potassium (^{40}K) and thorium (^{232}Th) mainly reflect the natural geological composition of the area.
- The spatial variations in radionuclide concentrations are attributed to differences in local geology, sedimentary deposits, and the redistribution of phosphate-bearing materials during historical mining activities.
- Mainly for potassium, it is naturally found in the soil and rocks.
- Uranium is mostly found in phosphate rocks from phosphate mines, and it was spread around when the mining was taking place.
- Thorium comes from old marine sands and their natural heavy minerals.

ACKNOWLEDGEMENTS

University of Venda

Stellenbosch
UNIVERSITY
IYUNIVESITHI
UNIVERSITEIT

DISCENDO ARMEMUS

REFERENCES

1. Bezuidenhout, J. 2015. In situ gamma ray measurements of radionuclides at a disused phosphate mine on the West Coast of South Africa. *Journal of Environmental Radioactivity*. 150:1–8. DOI: 10.1016/j.jenvrad.2015.07.030
2. Altfelder, S., van der Veeke, S., Hendriks, P.H.G.M. & Limburg, J., 2024. Scaling effects and integration of UAV and ground-based gamma-ray spectrometry data. *Journal of Environmental Radioactivity*, 264, p.107041.
3. Louw, I. 2020. Potential radiological impact of the phosphate industry in South Africa on the public and the environment (Paper 1). Journal of Environmental Radioactivity. 217:106214. DOI: 10.1016/j.jenvrad.2020.106214.
4. van der Veeke, S., Koomans, R. L., Limburg, J., de Waal, S. N., & van der Graaf, E. R. (2021). Optimising gamma-ray spectrometers for UAV-borne surveys with geophysical applications. Journal of Environmental Radioactivity, 235, 106649. https://doi.org/10.1016/j.jenvrad.2021.106649
5. International Atomic Energy Agency. (2024). Uranium exploration Planning, management and practice. In *IAEA TECDOC SERIES*. https://www-pub.iaea.org/MTCD/Publications/PDF/TE-2074web.pdf
6. Pinto, L.R., Vale, A., Brouwer, Y., Borbinha, J., Ventura, R., Silva, A.M., Mourato, A., Marques, G., Romanets, Y., Sargento, S., & Gonçalves, B. (2021). Radiological scouting, monitoring and inspection using drones. Sensors, 21(9), 3143. https://doi.org/10.3390/s21093143
7. Preugschat, B., Kunze, C., Wiens, B., & Altfelder, S. (2022). Drone-based investigations of uranium mining legacies: An airborne gamma spectrometry method to support, inspect, and monitor mine closure processes. In M. Tibbett, A. B. Fourie, & G. Boggs (Eds.), Mine Closure 2022 (pp. 623–632). Australian Centre for Geomechanics. https://doi.org/10.36487/ACG_repo/2215_44
8. Carvalho, F. P., Oliveira, J. M., & Lopes, I. (2014). Radionuclides from past uranium mining in rivers and streams of Portugal. Journal of Environmental Radioactivity, 132, 46–57. https://doi.org/10.1016/j.jenvrad.2014.01.016
9. Martin, P., Dayani, A., van der Veeke, S. & Limburg, J., 2020. High-resolution UAV-borne gamma-ray spectrometry for mineral exploration. *Remote Sensing*, 12(20), p.3376.


Thank You For Listening
?
Any Questions?